

## Bactericidal Effect of Silica Gel-Supported Porphyrinatophosphorus(V) Catalysts on *Escherichia coli* under Visible-Light Irradiation

Yoshiyuki Fueda,<sup>\*1</sup> Hideshige Suzuki,<sup>2</sup> Yasuhiro Komiya,<sup>2</sup> Yuka Asakura,<sup>2</sup> Tsutomu Shiragami,<sup>2</sup> Jin Matsumoto,<sup>2</sup> Haruhiko Yokoi,<sup>2</sup> and Masahide Yasuda<sup>\*2</sup>

<sup>1</sup>Fuji Silysia Chemical Ltd., 16303-3 Kihara, Hichiya, Hyuga 883-0062

<sup>2</sup>Department of Applied Chemistry, Faculty of Engineering, University of Miyazaki, Gakuen-Kibanadai, Miyazaki 889-2192

Received March 23, 2006; E-mail: fueda@fuji-silysia.co.jp

Dihydroxo- and dimethoxo(tetraphenylporphyrinato)phosphorus(V) complexes ( $[\text{P}(\text{OR})_2\text{tpp}]^+$ ) were immobilized on silica-gel powder affording a visible-light driven photocatalyst ( $[\text{P}(\text{OR})_2\text{tpp}]/\text{SiO}_2$ ; **1**). Bactericidal effect of complexes **1a** (R = H) and **1b** (R = Me) on *Escherichia coli* were investigated under visible-light irradiation. In the case of complex **1a**, the amount of *E. coli* decreased linearly versus the irradiation time, showing that the bactericidal reaction obeyed zero-order kinetics. Adsorption of bacteria on the catalyst is thought to be a key pathway by analysis according to Michaelis–Menten's equation. Complex **1a** was more effective for sterilization than complex **1b**. Stabilities of the  $[\text{P}(\text{OR})_2\text{tpp}]^+$  immobilized on silica-gel beads (**2**) were investigated in aqueous  $\text{CaCl}_2$  and  $\text{NaCl}$  solutions. The elution of the  $[\text{P}(\text{OH})_2\text{tpp}]^+$  chromophore from complex **2a** (R = H) was faster than it was from complex **2b** (R = Me).

Photocatalytic reactions have received much attention as an environmentally conscious process for decomposing and eliminating various pollutants in water and air<sup>1,2</sup> and for sterilizing bacteria occurring in a living environmental field.<sup>3–5</sup> In order to develop an efficient sterilizing method using a visible-light driven photocatalyst, our attention has been focused on metalloporphyrins that have a strong absorption in the visible region.<sup>6–11</sup> However, metalloporphyrins are insoluble in aqueous solution. In previous studies, we immobilized dihydroxo(tetraphenylporphyrinato)antimony(V) on silica gel and have found that it effectively sterilizes *Escherichia coli*<sup>12</sup> and *Legionella pneumophila*<sup>13</sup> in aqueous solution under visible-light irradiation. However, antimony is a heavy metal and can potentially cause cancer.  $\text{Sb}_2\text{O}_3$  has been determined to be a carcinogenic substrate by the international agency research on cancer (IARC).<sup>14</sup> If antimony diffuses into a living environmental field, the accumulation of antimony in plants and animals must taken into account. Therefore, we have changed the primary metal of the complex from antimony to phosphorus and investigated the bactericidal activity of tetraphenylporphyrinato phosphorus(V) immobilized on silica gel, which has a strong oxidizing ability.<sup>15,16</sup>

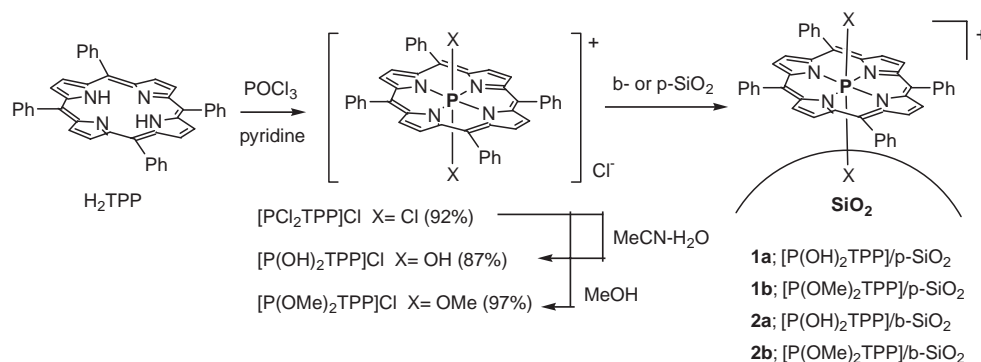
### Results and Discussion

**Preparation of the Catalyst.** According to the literature,<sup>17,18</sup> dichloro(tetraphenylporphyrinato)phosphorus(V) chloride complex ( $[\text{P}(\text{Cl})_2\text{tpp}]\text{Cl}$ ) was prepared by the reaction of tetraphenylporphyrin ( $\text{H}_2\text{tpp}$ ) with  $\text{POCl}_3$  in pyridine. The resulting  $[\text{P}(\text{Cl})_2\text{tpp}]\text{Cl}$  was converted into dihydroxo(tetraphenylporphyrinato)phosphorus(V) chloride ( $[\text{P}(\text{OH})_2\text{tpp}]\text{Cl}$ ) and dimethoxo(tetraphenylporphyrinato)phosphorus(V) chloride ( $[\text{P}(\text{OMe})_2\text{tpp}]\text{Cl}$ ) by solvolysis with  $\text{H}_2\text{O}$  and  $\text{MeOH}$ , respectively. Immobilization onto silica-gel powder ( $p\text{-SiO}_2$ ; 0.032–

0.045 mm $\phi$ ) was performed by refluxing  $[\text{P}(\text{OR})_2\text{tpp}]\text{Cl}$  in toluene with  $p\text{-SiO}_2$  for 18 h. The treated silica gel was filtered, and then dried under reduced pressure to give the  $p\text{-SiO}_2$ -supported  $[\text{P}(\text{OR})_2\text{tpp}]^+$  catalyst ( $[\text{P}(\text{OR})_2\text{tpp}]/p\text{-SiO}_2$ ; **1a** for R = H, **1b** for R = Me), in which the amount of the  $[\text{P}(\text{OR})_2\text{tpp}]^+$  chromophore was 0.42 wt % (Scheme 1).

$[\text{P}(\text{OR})_2\text{tpp}]\text{Cl}$  (R = H and Me) was fixed on silica-gel beads ( $b\text{-SiO}_2$ , 0.85–1.7 mm $\phi$ ) that were larger in particle size than  $p\text{-SiO}_2$  by refluxing in toluene– $\text{MeOH}$  solution (4:1 v/v). After filtration, the catalysts were washed with acetone and water to give the  $b\text{-SiO}_2$ -supported  $[\text{P}(\text{OH})_2\text{tpp}]^+$  catalyst ( $[\text{P}(\text{OH})_2\text{tpp}]/b\text{-SiO}_2$ ; **2a**) in which the content of the  $[\text{P}(\text{OH})_2\text{tpp}]^+$  chromophore was 0.042 wt %. In a similar manner,  $[\text{P}(\text{OMe})_2\text{tpp}]\text{Cl}$  was fixed on  $b\text{-SiO}_2$  to give the  $b\text{-SiO}_2$ -supported  $[\text{P}(\text{OMe})_2\text{tpp}]^+$  catalyst (**2b**). The catalysts were subjected to the stabilization experiments and the surface analysis.

**Photocatalytic Sterilization.** The bactericidal effect of complex **1a** was investigated using *E. coli* (K-12 IFO3335).<sup>12</sup> An aqueous phosphate buffer solution (10 cm<sup>3</sup>) containing *E. coli* (ca.  $10^4$  cell cm<sup>-3</sup>) and complex **1a** (10 mg) was introduced into L-type glass tubes and irradiated with a fluorescent lamp similar to the experiments involving the antimony analog ( $[\text{Sb}(\text{OH})_2\text{tpp}]/p\text{-SiO}_2$ ; **3**).<sup>12</sup> Upon irradiation in the presence of complex **1a**, the amount of *E. coli* decreased with an increase in irradiation time, as shown in Fig. 1. In contrast, in control experiments in the presence of complex **1a** under dark conditions and in the absence of a catalyst under irradiation, the amount of *E. coli* remained at 100% of the survival ratio. Thus, photocatalytic bactericidal activity of complex **1a** was confirmed. In addition, bactericidal experiments were performed at various concentrations of the catalyst ( $[\text{C}]$ ) under various light intensities ( $a$ ). The results are summarized in Table 1.



Scheme 1. Preparation of the photocatalyst.

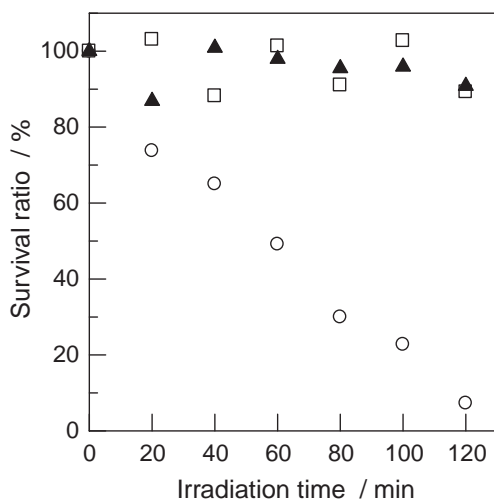


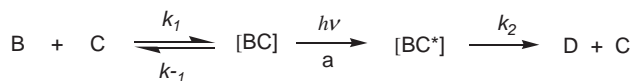
Fig. 1. Bactericidal experiment for *E. coli* in the presence of catalyst **1a** under irradiation by a fluorescent lamp (○), in the absence of a catalyst under irradiation (□), and in the presence of complex **1a** under dark conditions (▲): Initial concentration of *E. coli* = ca.  $1.0 \times 10^4$  cell  $\text{cm}^{-3}$ , [**1a**] =  $1.0 \text{ g dm}^{-3}$ , light intensity =  $21 \text{ W cm}^{-2}$ .

**Kinetic Analysis.** As a working hypothesis, we postulated that a Michaelis–Menten-type mechanism, which involves the interaction between bacteria and the catalyst in the ground state was occurring (Scheme 2). Based on Scheme 2, the bactericidal reaction rate ( $v$ ) is represented by Eq. 1,

$$v = k_2 a [\text{B}][\text{C}] / (K_m + [\text{B}]), \quad (1)$$

where  $K_m$  and  $a$  values represent  $(k_{-1} + k_2)/k_1$  and light intensity, respectively. The plots of the survival ratio of bacteria against the irradiation time at a given amount of complex **1a** showed a good straight line (Fig. 1). The reaction rates are independent of the concentration of bacteria  $[\text{B}]$ , and therefore, the bactericidal reaction obeys zero-order kinetics.

If the adsorption process of bacteria on the catalyst is very fast, i.e.,  $k_1$  is much larger than  $k_{-1}$  and  $k_2$ , the reaction rate ( $v$ ) equals  $ak_2[\text{C}]$  (Eq. 2). Since the  $[\text{P(OH)}_2\text{tp}]^+$  chromophore is cationic and  $\text{SiO}_2$  has an affinity for bacteria, a strong interaction between the catalyst and the bacteria was expected. Therefore, Eq. 2 can be transformed into Eq. 3 where  $[\text{B}_0]$  represents the initial concentration of *E. coli*. Actually, the plots with lower amounts of  $[\text{B}_0] - [\text{B}]$  against the irradiation time



Scheme 2. Possible mechanism. B: living cells, C: catalyst, D: deactivated cells, a: light intensity.

( $t$ ) gave a linear correlation until the conversion reached 75%, as shown in Fig. 2. The apparent rate constant ( $k_2$ ) can be derived from the slope of the plot which equals  $ak_2[\text{C}]$  (Eq. 4). As shown in Fig. 3, the plots of the slope vs  $a[\text{C}]$  gave a straight line with a slope equal to  $k_2$  which was determined to be  $2.14 \text{ min}^{-1}$ . In a similar way, the  $k_2$  value was determined to be  $1.10$  and  $4.40 \text{ min}^{-1}$  for complexes **1b** and **3**, respectively. Therefore, the catalytic reactivity increased in order of complexes **1b** < **1a** < **3**.

$$v = -d[\text{B}]/dt = k_2 a [\text{C}], \quad (2)$$

$$[\text{B}_0] - [\text{B}] = k_2 a [\text{C}] t, \quad (3)$$

$$\text{slope} = k_2 a [\text{C}]. \quad (4)$$

As mentioned above, the adsorption of *E. coli* on the catalyst is a key process. The  $[\text{P(OH)}_2\text{tp}]^+$  itself may have a strong affinity for the bacteria, and so, we studied the sterilization of *E. coli* with  $[\text{P(OH)}_2\text{tp}]\text{Cl}$  in an aqueous buffer solution. The plots of  $[\text{B}_0] - [\text{B}]$  vs irradiation time produced a straight line similar to that of the catalyst **1a** (Fig. 4). Therefore, the cationic  $[\text{P(OH)}_2\text{tp}]^+$  chromophore itself strongly interacts with the bacteria, which is why effective sterilization occurred.

**Mechanism.** Under  $\text{N}_2$ , photochemical sterilization using complex **1b** did not occur (Fig. 5B). Therefore, activated oxygen appears to participate in the sterilization process involving complex **1b**. Hirakawa et al. have reported that the photochemical damage of DNA occurred with  $[\text{Sb(OH)}_2\text{tp}]^+$  due to singlet oxygen ( $^1\text{O}_2$ ) which was generated by energy transfer from the excited triplet state of  $[\text{Sb(OH)}_2\text{tp}]^+$  to  $\text{O}_2$ .<sup>19</sup> In the present case, therefore, the bactericidal effect of complex **1b** was mainly attributed to activated oxygen involving  $^1\text{O}_2$ . In contrast, complex **1a** exhibited considerable bactericidal effects in the absence of  $\text{O}_2$ , as shown in Fig. 5A. Another reaction pathway through the interaction of the axial hydroxo ligand with the bacteria may also be involved in the case of complex **1a**.

**Stability of the Catalyst.** A catalyst must be stable in or-

Table 1. Photocatalytic Sterilization Using Complex **1a**

$a^a$	$[C]^b$	$a[C]$	Amount of cell (B)/ $10^3$ cell $\text{cm}^{-3}$							slope
			Time/min = 0	20	40	60	80	100	120	
21.0	0	0	7.77	7.64	7.60	7.58	7.67	7.58	7.54	1.3
21.0	0.1	2.1	8.27	8.11	7.60	7.38	7.21	7.06	6.79	12.8
21.0	0.5	10.5	7.75	7.02	6.57	6.06	5.75	5.29	4.93	25.4
21.0	1.0	21.0	7.60	6.36	5.38	3.95	2.60	1.32	0.50	60.9
21.0	2.0	42.0	7.76	6.05	4.41	1.42	0.22	0.02	0	96.0
21.0	3.0	63.0	8.57	6.37	3.34	0.63	0.06	0.01	0	126.0
7.3	1.0	7.3	4.97	4.64	4.34	4.01	3.86	3.54	3.31	14.3
11.0	1.0	11.0	5.14	4.90	4.39	3.97	3.73	3.25	2.66	19.4
17.0	1.0	17.0	5.20	4.75	4.04	3.50	3.07	1.98	1.25	30.9
20.3	1.0	20.3	5.56	4.66	3.74	2.31	1.83	1.24	0.24	43.8
25.6	1.0	25.6	5.79	4.50	3.55	2.40	0.92	0.30	0.05	59.0
21.0	2.0 <sup>c</sup>	42.0	5.42	5.44	4.83	3.96	2.62	1.20	0.22	46.0
21.0	1.0 <sup>d</sup>	21.0	10.31	7.25	5.81	4.44	2.47	1.21	0.66	92.5
21.0	$5 \times 10^{-7}$ <sup>e</sup>		5.28	5.11	4.25	3.83	2.62	1.64	0.86	39.0
21.0	$1 \times 10^{-6}$ <sup>e</sup>		5.92	4.50	4.32	3.27	1.88	0.87	0.48	50.0

a) Light intensity ( $a$ ) in  $\text{W cm}^{-2}$ . b) Concentration of catalyst  $[C]$  in  $\text{g dm}^{-3}$ . c) Using complex **1b**. The  $k_2$  value was determined to be  $1.10 \text{ min}^{-1}$ . d) Using complex **3**. The  $k_2$  value was determined to be  $4.40 \text{ min}^{-1}$ . e) Using aqueous  $[\text{P}(\text{OH})_2\text{tpp}]\text{Cl}$  solution ( $\text{mol dm}^{-3}$ ).

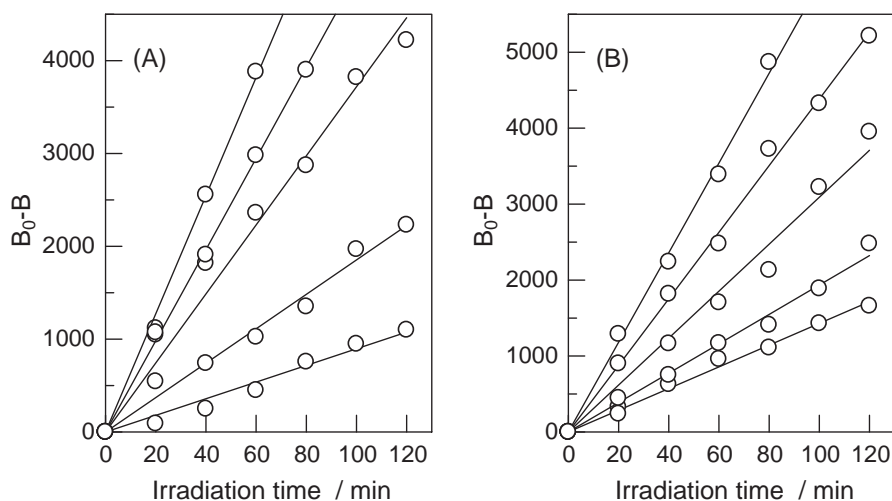


Fig. 2. Plots of  $[B_0] - [B]$  against the irradiation time ( $t$ ) (A) in the presence of a given amount of catalyst **1a** (0.1, 0.5, 1.0, 2.0, and  $3.0 \text{ g dm}^{-3}$ ) under irradiation with a light intensity of  $21 \text{ W cm}^{-2}$  and (B) in the presence of  $1 \text{ g dm}^{-3}$  of catalyst **1a** under various light intensities ( $a = 7.3, 11.0, 17.0, 20.3$ , and  $25.6 \text{ W cm}^{-2}$ ).

der to use it in practical applications. The catalysts (**2**;  $15.1 \text{ mg}$ ) were stored in aqueous solutions of  $\text{NaCl}$  and  $\text{CaCl}_2$  ( $0.1 \text{ mol dm}^{-3}$ ;  $20 \text{ cm}^3$ ) and distilled water ( $20 \text{ cm}^3$ ) at room temperature. Time-course plots are shown in Fig. 6. The amount of the  $[\text{P}(\text{OH})_2\text{tpp}]^+$  chromophore eluted from the catalyst was measured by its absorbance in UV-vis spectra of the aqueous solutions. The eliminated porphyrin chromophore was determined to be the  $[\text{P}(\text{OH})_2\text{tpp}]^+$  complex and not to be the free-base tetraphenylporphyrin ( $\text{H}_2\text{tpp}$ ). In the case of complex **2a**, the amount of the  $[\text{P}(\text{OH})_2\text{tpp}]^+$  chromophore in the aqueous solution gradually increased as the elution time increased. In particular,  $>80\%$  of the  $[\text{P}(\text{OH})_2\text{tpp}]^+$  chromophore was

eliminated after one month in the aqueous  $\text{NaCl}$  and  $\text{CaCl}_2$  solutions. However, the elution of the  $[\text{P}(\text{OMe})_2\text{tpp}]^+$  chromophore from complex **2b** was less than  $20\%$  after elution for 35 days, as shown in Fig. 6. We have already determined that deprotonation of an axial  $\text{O-H}$  ligand of  $[\text{P}(\text{OH})_2\text{tpp}]^+$  occurs, especially under irradiation.<sup>20–22</sup> Therefore, because the deprotonation causes the complex to become neutral, the elimination from complex **2a** was accelerated compared to that from complex **2b** (Scheme 3).

Although the total amount of the  $[\text{P}(\text{OMe})_2\text{tpp}]^+$  chromophore did not appreciably change in the case of complex **2b** in the elution experiments over a few weeks (Fig. 7), confocal

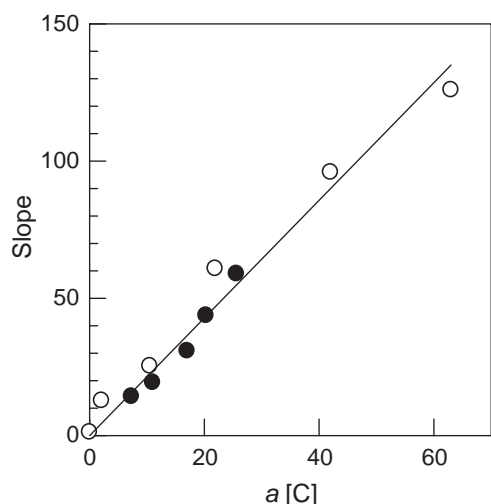


Fig. 3. Plots of the slopes vs the value of  $a[C]$  in the bactericidal experiments, using complex **1a** at the constant  $[C]$  (●) or the constant  $a$  (○). The slope is  $2.14 \text{ min}^{-1}$ .

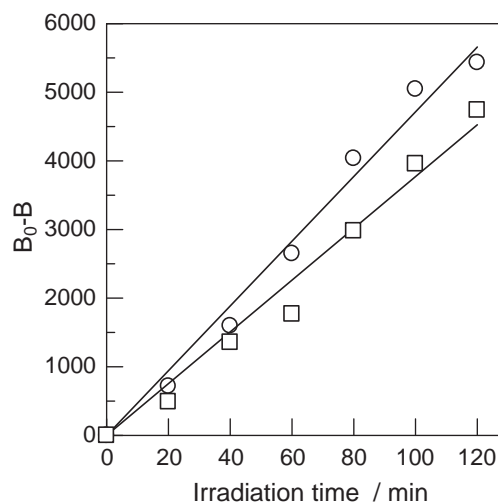


Fig. 4. Plots of  $B_0 - B$  vs irradiation time using  $[\text{P}(\text{OH})_2\text{tpp}]\text{Cl}$  whose concentrations were  $1 \times 10^{-6}$  (○) and  $5 \times 10^{-7} \text{ mol dm}^{-3}$  (□); initial concentration of *E. coli* =  $5.6 \times 10^3 \text{ cell cm}^{-3}$ ; light intensity =  $21 \text{ W cm}^{-2}$ .

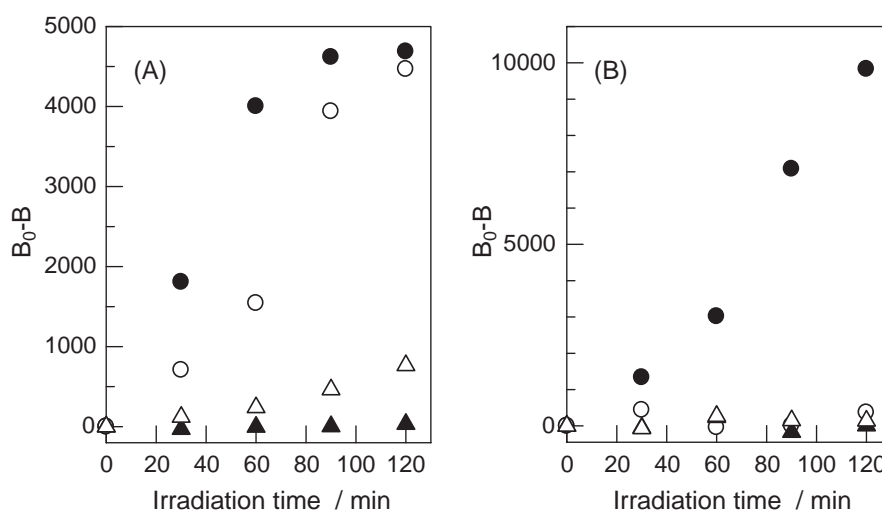


Fig. 5. Photochemical sterilization of *E. coli* by (A) complex **1a** and (B) complex **1b** in the presence of visible light under an oxygen atmosphere (●) and under a nitrogen-saturated atmosphere (○) and in the dark condition under an oxygen atmosphere (▲) and a under nitrogen-saturated atmosphere (△).

laser scanning microscope (CLSM) analysis showed that the fluorescence coming from the shallow part (100  $\mu\text{m}$  inside the surface) of complex **2b** was getting weaker as elution time increased (Fig. 7). In contrast, the fluorescence intensity from the deep part (400  $\mu\text{m}$  inside) of the catalyst did not decrease appreciably. Moreover, a dimple appeared on the silica-gel surface after the stability experiment in aqueous  $\text{CaCl}_2$  and  $\text{NaCl}$  solutions, suggesting the elimination of  $\text{SiO}_2$ .

In conclusion,  $[\text{P}(\text{OR})\text{tpp}]/\text{SiO}_2$  catalysts with high stability and non-toxicity, i.e., lethal dose 50 (LD50) of  $[\text{P}(\text{OH})_2\text{tpp}]\text{Cl} > 2000 \text{ mg kg}^{-1}$ , showed remarkable bactericidal activity towards *E. coli* under visible-light irradiation. Thus, it is expected that the present visible-light bactericidal technique will contribute to the practical sterilization of harmful microbes in aquatic bodies.

## Experimental

**Instruments.**  $^1\text{H}$ NMR spectra were taken on a Bruker AC 250P spectrometer. SIMS spectra were obtained on a Hitachi M2000A spectrometer. Microscopic spectroscopy was performed on an Olympus FV-300 confocal laser scanning microscope (CLSM) equipped with a spectrophotometer (STFL 250, Seki Technotron) linked to CLSM with an optical fiber.

**Materials. Preparation of Dialkylxo(tetraphenylporphyrinato)phosphorus(V) Chloride:** According to previous literature,<sup>17,18</sup> dichloro(tetraphenylporphyrinato)phosphorus(V) chloride,  $[\text{P}(\text{Cl}_2\text{tpp})\text{Cl}]$ , was prepared by the reaction of tetraphenylporphyrin (250 mg;  $\text{H}_2\text{tpp}$ ) and  $\text{POCl}_3$  (5  $\text{cm}^3$ ) in pyridine (50  $\text{cm}^3$ ) at reflux until the Soret band of the porphyrin shifted from 416 to 438 nm in UV spectra. After cooling, the reactant was pored into

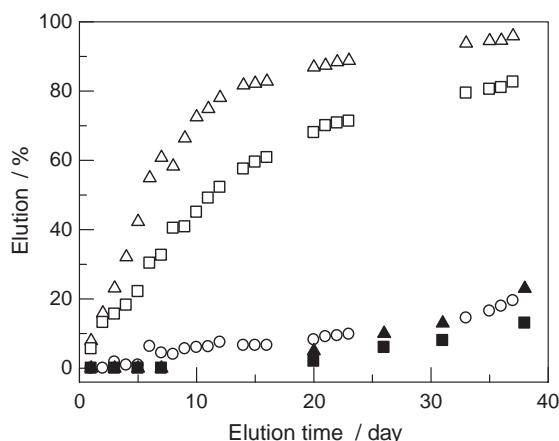


Fig. 6. Time-course plots of the amount of  $[P(OH)_2tpp]^+$  eluted from complex **2a** in the aqueous  $CaCl_2$  solution ( $\Delta$ ), aqueous  $NaCl$  solution ( $\square$ ), and distilled water ( $\circ$ ) and from complex **2b** in the aqueous  $CaCl_2$  solution ( $\blacktriangle$ ) and aqueous  $NaCl$  solution ( $\blacksquare$ ). The amounts were determined by UV-vis spectrometer using the absorption coefficient of the  $[P(OH)_2tpp]$  chromophore at 424 nm ( $\epsilon = 1.17 \times 10^5 \text{ dm}^3 \text{ mol}^{-1} \text{ cm}^{-1}$ ).

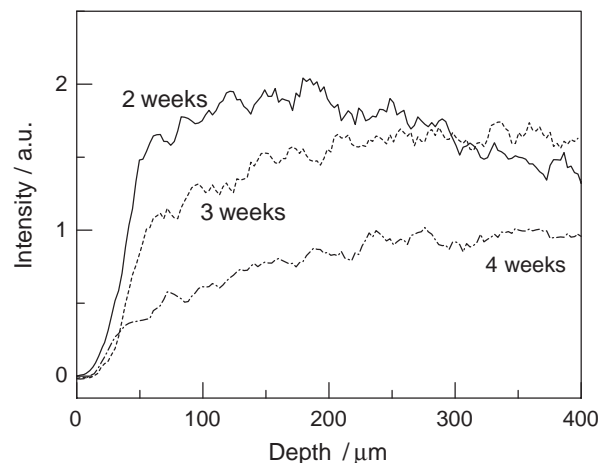
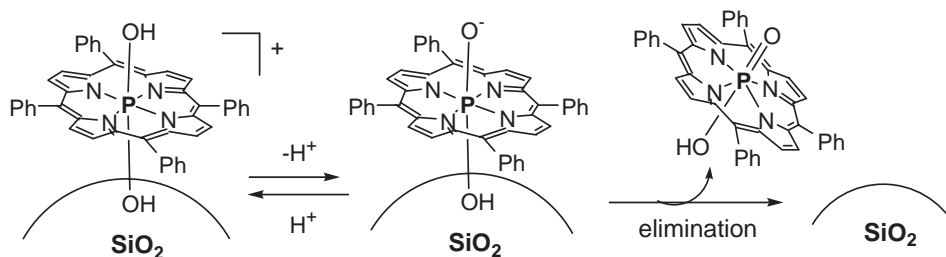


Fig. 7. Distribution of fluorescence in depth from the surface of complex **2b** after the elution experiment for a given periods.



Scheme 3. Plausible mechanism for elimination.

hexane (700  $\text{cm}^3$ ). The resulting precipitate was collected and dissolved in  $\text{CHCl}_3$  and washed with water. Crude  $[P\text{Cl}_2tpp]\text{Cl}$  was obtained from the  $\text{CHCl}_3$  solution after evaporation.

An  $\text{MeCN-H}_2\text{O}$  (3:1, 160  $\text{cm}^3$ ) solution of  $[P\text{Cl}_2tpp]\text{Cl}$  (250 mg) was heated at reflux until the Soret band shifted from 436 to 423 nm in UV spectra. After evaporation of the MeCN, the aqueous solution was extracted with  $\text{CHCl}_3$ . The  $\text{CHCl}_3$  extracts were combined and the  $\text{CHCl}_3$  was evaporated to give dihydroxo(tetraphenylporphyrinato)phosphorus(V) chloride,  $[P(OH)_2tpp]\text{Cl}$  (87% yield). A MeOH (250 mL) solution of  $[P\text{Cl}_2tpp]\text{Cl}$  (150 mg) was heated at reflux until the Soret band shifted from 435 to 424 nm in UV spectra.  $[P(\text{OMe})_2tpp]\text{Cl}$  was obtained (97% yield) after work up similar to that of  $[P(OH)_2tpp]\text{Cl}$ .

$[P\text{Cl}_2tpp]\text{Cl}$ .<sup>18</sup> 92% yield.  $\lambda_{\text{max}}$  ( $\log \epsilon$ )/nm 435 (4.54).  $^1\text{H NMR}$   $\delta$  7.77–7.82 (m, 12H), 7.97–8.01 (m, 8H), 9.14 (d,  $J_{\text{P-H}} = 4.52 \text{ Hz}$ , 8H). SIMS  $m/z = 735$  ( $P\text{Cl}_2tpp$ ).

$[P(OH)_2tpp]\text{Cl}$ .<sup>20</sup> 87% yield.  $\lambda_{\text{max}}$  ( $\log \epsilon$ )/nm 423 (4.51).  $^1\text{H NMR}$   $\delta$  7.67–7.70 (m, 12H), 7.99–8.03 (m, 8H), 8.80 (d,  $J_{\text{P-H}} = 1.93 \text{ Hz}$ , 8H). SIMS  $m/z = 676$  ( $P(OH)_2tpp - 2\text{H}$ ).

$[P(\text{OMe})_2tpp]\text{Cl}$ .<sup>18</sup> 97% yield.  $\lambda_{\text{max}}$  ( $\log \epsilon$ )/nm 424 (4.16).  $^1\text{H NMR}$   $\delta$  -1.87 (d,  $J_{\text{P-H}} = 25.7 \text{ Hz}$ , 6H), 7.74–7.81 (m, 12H), 7.92–7.95 (m, 8H), 9.07 (d,  $J_{\text{P-H}} = 2.7 \text{ Hz}$ , 8H). SIMS  $m/z = 706$  ( $P(\text{OMe})_2tpp$ ).

**Preparation of  $\text{SiO}_2$ -Supported (Tetraphenylporphyrinato)-phosphorus Catalyst:** The  $[P(OH)_2tpp]\text{Cl}$  chromophore was supported on an  $\text{SiO}_2$  carrier. Two types silica gel were used:

Table 2. Characterization of the Catalyst

Catalyst	Chromophore/wt %	Support <sup>a)</sup>
<b>1a</b>	$[P(OH)_2tpp]\text{Cl}$ (0.42)	<i>p</i> - $\text{SiO}_2$
<b>1b</b>	$[P(\text{OMe})_2tpp]\text{Cl}$ (0.42)	<i>p</i> - $\text{SiO}_2$
<b>2a</b>	$[P(OH)_2tpp]\text{Cl}$ (0.042)	<i>b</i> - $\text{SiO}_2$
<b>2b</b>	$[P(\text{OMe})_2tpp]\text{Cl}$ (0.042)	<i>b</i> - $\text{SiO}_2$
<b>3</b>	$[\text{Sb}(\text{OH})_2tpp]\text{Br}$ (0.87)	<i>p</i> - $\text{SiO}_2$

a) *p*- $\text{SiO}_2$ : powder-type silica gel, size: 0.032–0.045 mm $\phi$ , surface area: 429  $\text{m}^2 \text{ g}^{-1}$ . *b*- $\text{SiO}_2$ : beads-type silica gel, size: 1.70–4.00 mm $\phi$ , surface area: 306  $\text{m}^2 \text{ g}^{-1}$ .

silica-gel powders (*p*- $\text{SiO}_2$ ; 300 mesh, 0.04 mm $\phi$ , 30 g, BW300, Fuji Silysia Chemical Ltd., Japan) and silica-gel beads (*b*- $\text{SiO}_2$ ; 0.85–1.70 mm $\phi$ , 30 g, CARIAC T Q-10, Fuji Silysia Chemical Ltd., Japan) (Table 2).

Into a toluene solution (400  $\text{cm}^3$ ) of  $[P(OH)_2tpp]\text{Cl}$  or  $[P(\text{OMe})_2tpp]\text{Cl}$  (132 mg), *p*- $\text{SiO}_2$  (30 g) was added, and then the solution was refluxed for 18 h. The treated silica gel was filtered, and then dried under reduced pressure to give catalysts **1a** and **1b**, respectively, in which the content of the  $[P(\text{OR})_2tpp]^+$  chromophore was 0.42 wt %.

A toluene–MeOH solution (4:1 v/v, 200  $\text{cm}^3$ ) of  $[P(OH)_2tpp]\text{Cl}$  or  $[P(\text{OMe})_2tpp]\text{Cl}$  (13.2 mg) was refluxed with *b*- $\text{SiO}_2$  (30 g), filtered, and then washed with acetone and water (100  $\text{cm}^3$ ) to give



catalysts **2a** and **2b**, respectively, in which the content of the  $[\text{P}(\text{OR})_2\text{tpp}]^+$  chromophore was 0.042 wt %.

The catalysts were characterized by observation of characteristic fluorescence peaks<sup>23,24</sup> using CLSM.

**Photocatalytic Sterilization of *E. coli* in an L-Type Glass Tube.** The amount of *E. coli* was adjusted to ca.  $10^4$  cell  $\text{cm}^{-3}$  by counting with a microscope. The bactericidal activities of catalyst **1** on *E. coli* were examined in an L-type glass tube similar to the previously reported method.<sup>12</sup> Catalyst **1** (10 mg),  $1.0 \text{ cm}^3$  of the *E. coli* cell suspension, and  $9.0 \text{ cm}^3$  of phosphate buffer ( $100 \text{ mmol dm}^{-3}$ , pH 7.0) were added into an L-type glass tube (length 18 cm, diameter 1.5 cm). The L-type glass tube was set on a reciprocal shaker and irradiated with two fluorescent lamps set above the shaker. The reaction temperature was kept constant at  $30^\circ\text{C}$ . A portion ( $0.1 \text{ cm}^3$ ) of the solution was plated on the basal medium supplemented with 20 g agar  $\text{dm}^{-3}$ , after which the colonies that appeared after 14 h of incubation at  $30^\circ\text{C}$  were counted for three replicate plates.

**Stability of Catalysts 2.** The catalysts (**2**; 15.1 mg) were immersed in aqueous NaCl and  $\text{CaCl}_2$  ( $0.1 \text{ mol dm}^{-3}$ ;  $20 \text{ cm}^3$ ) solutions and distilled water ( $20 \text{ cm}^3$ ) at room temperature. For each sampling,  $10 \text{ cm}^3$  of the solution was taken and subjected to UV-vis spectroscopy. After UV measurement, additional amounts of aqueous NaCl and  $\text{CaCl}_2$  ( $0.1 \text{ mol dm}^{-3}$ ;  $10 \text{ cm}^3$ ) solutions and distilled water ( $10 \text{ cm}^3$ ) were added to the original solutions to keep the amounts at  $20 \text{ cm}^3$  and to maintain the stability experiment.

This work was supported by a Cooperative Project of Miyazaki prefecture, Japan and partially by a Grand-in-Aid for Scientific Research (No. 14050079, Scientific Research in Priority Areas 417) from the Ministry of Education, Culture, Sports, Science and Technology.

## References

- 1 O. Legrini, E. Iliveros, A. M. B. Braun, *Chem. Rev.* **1993**, 93, 671.
- 2 J. Theurich, M. Lindner, D. W. Bahnemann, *Langmuir* **1996**, 12, 6368.
- 3 T. Matsunaga, R. Tomoda, T. Nakajima, H. Wake, *FEMS Microbiol. Lett.* **1985**, 29, 211.
- 4 T. Saito, T. Iwase, J. Horie, T. Morioka, *J. Photochem. Photobiol., B* **1992**, 14, 369.
- 5 C. Wei, W. Y. Lin, Z. Zainai, N. E. Williams, K. Zhu, A. P. Kruzic, R. L. Smith, K. Rajeshwar, *Environ. Sci. Technol.* **1994**, 28, 934.
- 6 *Homogeneous and Heterogeneous Photocatalysis*, ed. by A. Harriman, P. Neta, M. C. Richoux, E. Pelizzetti, N. Serpone, D. Reidel Pub. Co., Dordrecht, The Netherlands, **1986**, p. 123, and references cited therein.
- 7 S. Takagi, T. Okamoto, T. Shiragami, H. Inoue, *J. Org. Chem.* **1994**, 59, 7373.
- 8 T. Shiragami, K. Kubomura, D. Ishibashi, H. Inoue, *J. Am. Chem. Soc.* **1996**, 118, 6311.
- 9 H. Inoue, S. Funyu, Y. Shimada, S. Takagi, *Pure Appl. Chem.* **2005**, 77, 1019.
- 10 T. Shiragami, Y. Shimizu, K. Hinoue, Y. Fueda, K. Nobuhara, I. Akazaki, M. Yasuda, *J. Photochem. Photobiol., A* **2003**, 156, 115.
- 11 T. Shiragami, R. Makise, Y. Inokuchi, J. Matsumoto, H. Inoue, M. Yasuda, *Chem. Lett.* **2004**, 33, 736.
- 12 H. Yokoi, T. Shiragami, J. Hirose, T. Kawauchi, K. Hinoue, Y. Fueda, K. Nobuhara, I. Akazaki, M. Yasuda, *World J. Microbiol. Biotechnol.* **2003**, 19, 559.
- 13 Y. Fueda, M. Hashimoto, K. Nobuhara, H. Yokoi, Y. Komiya, T. Shiragami, J. Matsumoto, K. Kawano, S. Suzuki, M. Yasuda, *Biocontrol Sci.* **2005**, 10, 55.
- 14 IARC Monogr. Eval. Carcinog. Risks Hum. **1989**, 47, 291.
- 15 C. A. Marrese, C. J. Carrano, *Inorg. Chem.* **1983**, 22, 1858.
- 16 Y. Yamamoto, K.-y. Akiba, *J. Organomet. Chem.* **2000**, 611, 200.
- 17 R. P. Pandian, T. K. Chandrasekhar, V. Chandrasekhar, *Indian J. Chem., Sect. A* **1991**, 30, 579.
- 18 H. Segawa, K. Kunimoto, A. Nakamoto, T. Shimidzu, *J. Chem. Soc., Perkin Trans. 1* **1992**, 939.
- 19 K. Hirakawa, S. Kawanishi, J. Matsumoto, T. Shiragami, M. Yasuda, *J. Photochem. Photobiol., B* **2006**, 82, 37.
- 20 Y. Andou, K. Ishikawa, K. Shima, T. Shiragami, M. Yasuda, *Bull. Chem. Soc. Jpn.* **2002**, 75, 1757.
- 21 Y. Yamamoto, R. Nadano, M. Itagaki, K.-y. Akiba, *J. Am. Chem. Soc.* **1995**, 117, 8287.
- 22 K. Kunimoto, H. Segawa, T. Shimidzu, *Tetrahedron Lett.* **1992**, 33, 6327.
- 23 K. Susume, K. Kunimoto, H. Segawa, T. Shimidzu, *J. Phys. Chem.* **1995**, 99, 29.
- 24 T. A. Rao, B. G. Maiya, *Inorg. Chem.* **1996**, 35, 4829.